

Structuring laminar flows using annular magnetohydrodynamic actuation

Jonathan West^{a,*}, James P. Gleeson^b, John Alderman^a,
John K. Collins^c, Helen Berney^a

^a National Microelectronics Research Centre, Lee Maltings, Prospect Row, Cork, Ireland

^b Department of Applied Mathematics, NUI, Cork, Ireland

^c Department of Microbiology, NUI, Cork, Ireland

Received 19 December 2002; received in revised form 29 May 2003; accepted 5 June 2003

Abstract

Laminar flow behaviour is typically observed when transporting fluids in micron-scale channels. Here, cross channel mass transport occurs only by molecular diffusion and mixing adjacent fluid streams becomes problematic. A parabolic velocity profile is also observed with pressure-driven laminar flow in a conduit. This property can be exploited by circulating fluid in an annulus such that two initially separated liquids are forced to pass through each other resulting in massive increases in the interfacial area to promote conditions for mass transfer. Miniature machined and micromachined prototypes with an integrated magnetohydrodynamic (MHD) micropump for fluid circulation were fabricated and tested. Annular MHD micromixing was characterised using fluorescein, bromophenol blue and hydrogen ion solutes for a range of velocities and modelled to include both diffusive and convective components. Furthermore, a lateral partitioning mechanism was identified and examined.

© 2003 Elsevier B.V. All rights reserved.

Keywords: Microfluidics; Laminar flow; Magnetohydrodynamic (MHD) micropump; Annular micromixing; Transverse partitioning

1. Introduction

The miniaturisation of analytical and synthetic apparatus offers inherent gains in performance as a consequence of fundamental scaling laws. This approach also presents the possibility to exploit phenomena that do not exist in macroscopic systems, thereby increasing the repertoire of methods for chemical manipulation. The transport of fluids through these miniature systems is typically associated with a low Reynolds number, Re , where non-turbulent, or laminar flow behaviour dominates. Here, flows are predominantly uniaxial (i.e. moving parallel to the channel walls), where molecular diffusion is the only force to govern transverse flow (i.e. movement across the channel's width). This feature has found numerous applications, including diffusion controlled particle filtration [1], concentration gradient construction [2], and the measurement of reaction kinetics [3]. However, many processes require the homogenisation of chemical species, and the same diffusion limited transport

introduces unacceptably lengthy mixing timescales. Methods to enhance mixing are therefore required to overcome this hindrance. The incorporation of conventional moving stirrer elements in microdevices presents both a fabrication and reliability challenge, and has inspired investigation of other mixing mechanisms. By introducing convective forces with appropriate microchannel design, fluid interfaces can be significantly increased to enable thorough mixing by molecular diffusion. For example, microfabricated nozzles can be used for hydrodynamic focusing where a high velocity, high surface-to-volume ratio chemical stream is created to achieve mixing in microseconds [4]. Other ingenious solutions generate vortices using so-called herring bone microchannel surface modifications [5] or by using orthogonal alternating Lorentz forcing [6]. Another method involves the initiation of electrokinetic instabilities during electroosmotic flow to generate transverse flow components and thereby affect micromixing [7]. More commonly, however, microchannel interconnection and layout can be used to create multiple co-current flows with a high interfacial area for inter-stream diffusional mixing [8,9].

A parabolic velocity profile is typical of laminar flows in a channel. This characteristic can be coupled with an annular

* Corresponding author. Tel.: +353-21-4904225;

fax: +353-21-4270271.

E-mail address: jonathan.west@nmrc.ie (J. West).

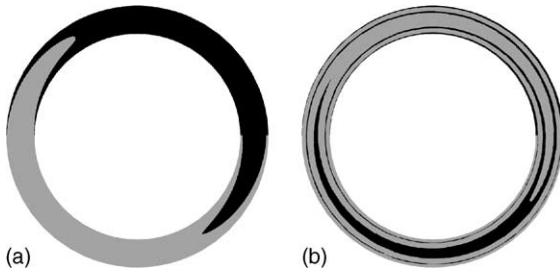


Fig. 1. The 2-D behaviour of two laminar flows in an annular micromixer after (a) ~ 0.125 and (b) ~ 1.625 revolutions at peak velocity. A zero diffusion condition is assumed.

geometry to provide an alternative method for micromixing. As shown in Fig. 1, a circulating and laminar flow causes two initially separated fluids to repeatedly pass through each other to create multiple lamellae with a high interfacial area for diffusion-mediated mixing. However, the actuation of fluids in an annular channel is not trivial. Fluid circulation using a magnetohydrodynamic (MHD) micropump does not suffer geometry restrictions and has previously been demonstrated as a means to address this [10,11]. MHD actuation is an electrically controllable, reversible, low power consumption fluid-drive method that obviates the use of moving parts by acting locally on the electrolyte, exploiting its inherent conductive nature. MHD propulsion is realised when an electric field operates in, and perpendicular to, a magnetic field [10,12]. This orthogonal arrangement generates a Lorentz force that is perpendicular to both electric and magnetic fields, and acts to induce fluid transport. Typically, MHD transport is achieved using a cross channel electric current in combination with a magnetic field originating from beneath the channel. Fluid manipulation using MHD propulsion has found several applications, including fluidic switching in a microfluidic network [13,14] and continuous flow chemistries [11]. Other approaches have exploited the Lorentz transport phenomenon to structure microscopic flow patterns [15]. In this paper, we report the use of MHD-driven uniaxial transport to stretch, fold and partition fluid streams circulating in a microscale annulus.

2. Experimental

2.1. Fabrication

Machined and microfabricated annular MHD devices were used to understand the behaviour of fluid circulating under a Lorentz force. The machined prototype was fabricated using a brass disc positioned within a brass ring (both $500\ \mu\text{m}$ -thick), and glued to a polycarbonate plate ($350\ \mu\text{m}$ -thick), to realise vertical channel walls that also serve as electrodes. The disc has a radius of $4\ \text{mm}$, and the ring has an internal radius of $6\ \text{mm}$, to create a $2\ \text{mm}$ -wide channel with a centre-line radius of $5\ \text{mm}$ and a depth of $500\ \mu\text{m}$, giving a volume of $\sim 32\ \mu\text{L}$. Dimensions were determined using digital Vernier callipers with an accuracy

of $\pm 10\ \mu\text{m}$. The device could be operated without a lid, or alternatively a transparent polycarbonate top plate was used to enclose the annulus. The micromachined device was fabricated using a $525\ \mu\text{m}$ -thick silicon substrate. A KOH etch was used to define an annulus to a depth of $150\ \mu\text{m}$. This anisotropic etch results in vertical walled regions ($1278\ \mu\text{m}$ wide), and 54° etch regions where the channels are wider at the top than the bottom (1045 and $830\ \mu\text{m}$, respectively), and still further regions where a combination of these cross-section geometries exist, resulting in an average width of $1160\ \mu\text{m}$ and an average internal radius of $4.42\ \text{mm}$, giving a volume of $\sim 5.5\ \mu\text{L}$. Following the growth of a $1\ \mu\text{m}$ -thick SiO_2 using a wet furnace (Thermco 9000 Furnace), the wafers were coated with metal ($350\ \text{\AA}$ Cr, $2000\ \text{\AA}$ Au) using a Temascal Evaporator (BJD1800). Standard photolithographic methods were used with Eagle electrophoretic negative photoresist (ED2100) to pattern metal electrodes on the channel walls [16]. During operation the annulus was enclosed with a $150\ \mu\text{m}$ -thick glass superstrate secured using capillary forces. The silicon device is depicted in Fig. 2.

2.2. MHD flow model

A mathematical model for annular MHD propulsion has previously been reported [17]. Briefly, the equations of incompressible MHD flow [18] may be reduced to a Navier–Stokes equation with a Lorentz force. Given a cylindrically symmetric geometry, and therefore circular streamlines, an exact reduction to a Poisson equation is possible. This can be solved by using a Fourier–Bessel expansion, or by straightforward numerical computation using a two-dimensional finite element package, where a zero-flux boundary condition ($v = 0$) is assumed and produces a parabolic velocity profile with a maximum towards the inner wall at half depth. Plotted in Fig. 3 is the non-dimensional quantity

$$-v(r, z) \times \left(\frac{BI}{4\pi h\eta} \right)^{-1} \quad (1)$$

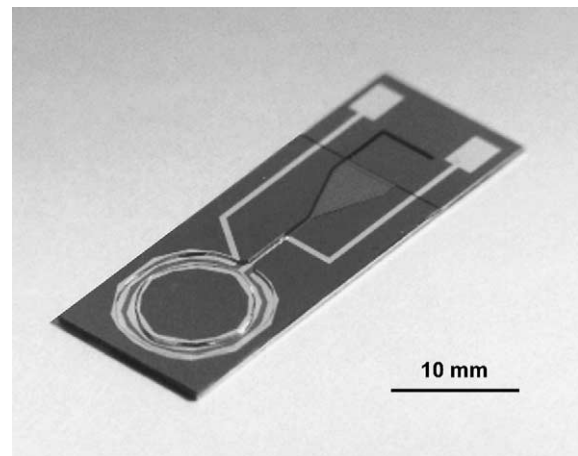


Fig. 2. MHD micromixer with an annular channel realised by KOH etching silicon, and with Cr/Au electrodes patterned on the channel walls.

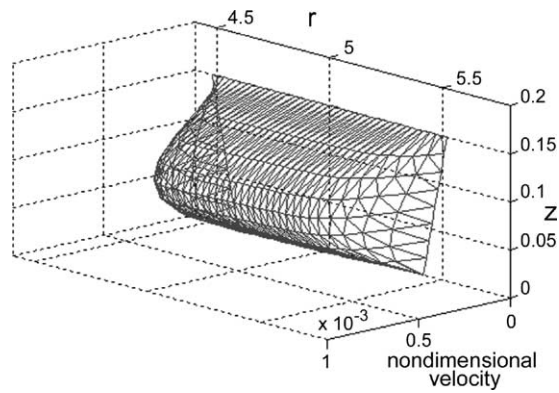


Fig. 3. Finite element solution for velocity profile in the silicon microreactor annulus at a region with a 54° etch. Depth is $150\ \mu\text{m}$ and measured along the vertical z -axis in μm . The channel width is $1045\ \mu\text{m}$ at the top and $830\ \mu\text{m}$ at the bottom of the channel, with channel radius measured in mm along the r -axis.

evaluated at each (r, z) point in the silicon channel cross-section, where r denotes the radius and z the depth. The force generated is the product of the magnetic B and electric I fields, with channel depth h and η denoting the fluid's viscosity. The non-dimensional multipliers used to find the average and peak velocities (by multiplication with the $BI/4\pi h\eta$ expression) in the silicon microreactor and the open and closed machined device are calculated from the Poisson solver and recorded in Table 1.

2.3. Apparatus and measurements

MHD actuation using a 1 kHz AC signal was implemented to avoid issues of net reactant migration leading to electrode and reactant degradation, and the accompanying electrolytic bubble generation, when operating in DC mode [10]. An elementary series circuit was used to synchronise sinusoidal electric and magnetic fields to generate a circulating Lorentz force. With this arrangement, the Lorentz force depends on the amplitude and oscillation state of the AC electric and magnetic fields. Thus, during one period of oscillation a variation in the magnitude of the Lorentz force is seen, resulting in a pulsatile flow where the peak force generated is double that of the time-averaged force. However, operation at high frequencies (1 kHz) with a viscous fluid generates a flow that can be effectively regarded as continuous, reflecting the time-averaged force [12].

The experimental apparatus comprised an AC power source (HP 6813A) connected in series to an MHD device and an electromagnet. In addition, the circuit incorporates a primitive trimmer made with a combination of parallel high power resistors (6 W, $470\ \Omega$) and switches to provide a method to differentially regulate the channel current in favour of the magnetic field. The electromagnet was fabricated using 350 turns of copper wire about a ferrite tube with a relative permeability, μ_r , of $800\ \text{H m}^{-1}$. This gives an inductance of 3.8 mH, such that the impedance is almost purely resistive at 1 kHz. The phase shift between the electric and magnetic states is therefore nearly equal to zero to enable field synchronisation for efficient MHD actuation with minimal ohmic heating. For a range of voltage inputs, multiple cover slips were used as spacers to provide $150\ \mu\text{m}$ intervals for magnetic field measurements using a magnetic probe (GM05 Gaussmeter, Hirst). During operation, the average magnetic field experienced by the fluid in the microchannels could therefore be determined as a function of the electromagnetic current. Flow velocities were extrapolated from Eq. (1) using cross-channel and electromagnet current measurements, where the viscosity and density were assumed to be that of water at a given temperature.

Aqueous KCl solutions (125 mM to 3 M) served as the electrolyte and were introduced to both devices by pipetting. Video microscopy tracking was used to determine fluid velocities in the machined and silicon devices by monitoring the transport of $\sim 100\ \mu\text{m}$ diameter polyvinylchloride (PVC) and $6\ \mu\text{m}$ diameter latex particles, respectively. Bromophenol blue (BPB) or fluorescein dyes have small diffusion coefficients ($\kappa \approx 3 \times 10^{-6}\ \text{cm}^2\ \text{s}^{-1}$ at 25°C) and were used to visualise the structuring of lamellae for several revolutions. Mixing experiments involved the dispensing of $3\ \mu\text{L}$ aliquots of 1 M KCl with 5 mM fluorescein or 10 mM BPB into the annulus containing 1 M KCl adjusted to pH 7.0, followed by MHD-driven fluid circulation. Upon homogeneity of the BPB tracer, a 500 nL aliquot of 500 mM HCl and 500 mM KCl was introduced, and the diffusion-limited reaction of H^+ with BPB was used to observe the mixing of a species with a high diffusion coefficient ($\kappa = 9.31 \times 10^{-5}\ \text{cm}^2\ \text{s}^{-1}$ at 25°C). Mixing was monitored at the initial dye front by video microscopy. Frames were recorded using Studio MP10 v.1.02 software (Pinnacle Systems), and analysed with IMAQTM Vision Builder v.6 software (National Instruments). A fibre optic was used to provide near-vertical

Table 1
Device geometries and non-dimensional multipliers

Device	Height (μm)	Width (μm)	Average multiplier (non-dimensional)	Peak multiplier (non-dimensional)
Machined (open)	500 ± 10	2000 ± 10	1.15×10^{-2}	2.31×10^{-2}
Machined (closed)	500 ± 10	2000 ± 10	3.50×10^{-3}	6.60×10^{-3}
Silicon microreactor	150	1160 average	3.30×10^{-4}	5.90×10^{-4}

Multiplication of these factors with the dimensional value of $BI/4\pi h\eta$ can be used to find peak and average transport velocities. Separate computation of the non-dimensional velocities at the two silicon microchannel cross-section extremes reveals only a 2% difference, and an average value is noted and used to calculate the transport velocity.

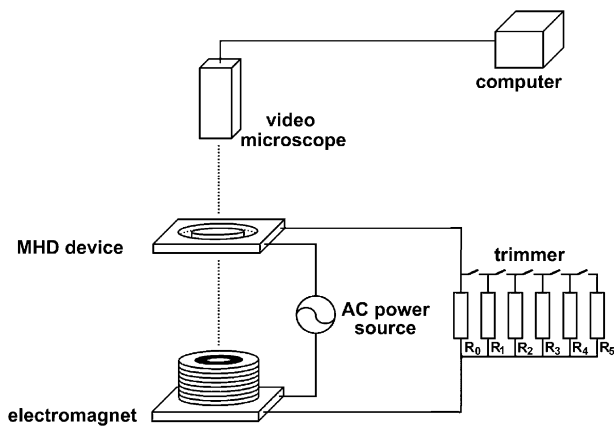


Fig. 4. Apparatus and experimental set-up (including the series circuit arrangement) for tracking particles and monitoring micromixing in the annular MHD microreactors.

illumination, and a coefficient of variation tolerance limit of 5% was introduced to accommodate the associated image variation (i.e. when the fluorescence variation reaches this level mixing is complete). Subtractive dichroic colour filters (Edmund Optics Ltd.) were used to excite fluorescein at 492 nm and observe emission at 520 nm. Mixing times for BPB, fluorescein, and H⁺ with BPB were recorded over a range of average velocities. The experimental set-up for annular MHD micromixing is depicted in Fig. 4.

3. Results and discussion

3.1. MHD actuation

Both machined and micromachined MHD systems were able to pump aqueous solutions doped with KCl as the charge carrier. Consistent with pressure-driven microfluidics, a Poiseuille flow was observed with zero movement at the channel surface and peak velocities at the channel centre. Particle velocities were found to cluster around the average predicted by the relevant model, with peak velocities in close agreement with the modelled values. Model predictions for the different MHD micropumps are compared with observed velocities in Table 2. Furthermore, it is observed that (for a given electrode voltage) the value of the current I changes proportionally with channel height h to maintain the current density. Consequently the $BI/4\pi h\eta$

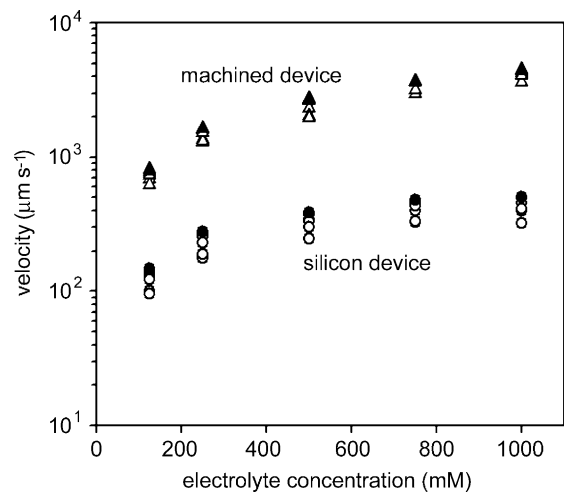


Fig. 5. Modelled (solid symbols) and observed peak velocities (empty symbols) of MHD-driven fluid streams as a function of electrolyte concentration in the open machined device (triangles) and the micromachined silicon device (circles). Experiments were conducted using particle-doped KCl (aq) at room temperature (~25 °C) where the absolute viscosity η is $0.9 \times 10^{-3} \text{ kg m}^{-1} \text{ s}^{-1}$. Data points are recorded for five particles moving at the centre of the microchannel under the same actuation conditions (6.5 Vrms, 1 kHz circuit signal) and for a given KCl concentration.

factor in (1) is unaltered, and the actuation velocity therefore effectively scales in accordance with the non-dimensional multiplier by h^2 [11].

The generation of a Lorentz force is dependent on the availability of charge carriers (e.g. ions) in the fluid. Increasing the electrolyte concentration provides conductivity gains and was therefore found to generate higher cross-channel currents. In addition, the series circuit acts to provide gains in the magnetic field when the channel current is increased. These inputs combine to create Lorentz forces, and pumping velocities, that increase with an increase in the electrolyte concentration. MHD actuation would therefore be favoured for applications involving concentrated electrolytes with large ionic mobilities, or even ionic liquids, where pumping methods such as electroosmotic flow are compromised [19]. Shown in Fig. 5, this relationship is revealed for KCl concentrations ranging from 125 mM to 1 M, and compared with peak velocities generated by the model. Occasional deviation above the modelled peak velocity could be attributed to channel imperfections associated with machining, or ohmic heating during prolonged actuation with a high electrolyte concentration. Alternatively, the same gains

Table 2
The performance of the machined and the silicon MHD micropumps

Device type	Peak channel current (mA)	Peak magnetic field (mT)	Modelled velocity average (mm s^{-1})	Modelled velocity peak (mm s^{-1})	Observed velocity average (mm s^{-1})	Observed velocity peak (mm s^{-1})
Machined (open)	121	9.3	2.229	4.597	2.548	4.661
Machined (closed)	111	8.7	0.570	1.140	0.545	1.088
Silicon	141	10.2	0.281	0.502	0.265	0.498

Experiments were conducted using 1 M KCl (aq) at room temperature (~25 °C) where the absolute viscosity η is $0.9 \times 10^{-3} \text{ kg m}^{-1} \text{ s}^{-1}$. Observed velocity averages were calculated using data from 20 particles moving under the same actuation conditions (6.5 Vrms, 1 kHz circuit signal).

in velocity can be realised by the application of higher circuit voltages (data not shown).

The application of a voltage through a solvent and across miniature distances is associated with electrolysis and the accompanying formation of bubbles and a drop in the channel current. This effect can be reduced by the application of an AC signal, but still imposes actuation limits. When operating with a 1 M KCl electrolyte and a 1 kHz signal, the electrode voltage electrolysis threshold was found to be ~ 9.8 and 4.9 V_{rms}, in the machined and silicon micropumps, respectively. At this voltage limit, the open machined device was capable of pumping a 1 M KCl electrolyte at a peak velocity of ~ 18 mm s⁻¹, with a volumetric flow rate in excess of 500 μ L min⁻¹. The silicon device, however, demonstrates more modest pumping performance as a consequence of both the voltage and channel depth limitations. Here, maximal velocities of the order of 0.6 mm s⁻¹ and volumetric flow rates of 3.1 μ L min⁻¹ were achieved when mobilising the same electrolyte.

3.2. Annular micromixing model

The mixing of co-current streams involves both uniaxial convective motion and diffusive transport components and can be described using a Peclet number ($Pe = U\ell/\kappa$, where U is the average flow speed, ℓ the smallest spatial dimension and κ the diffusion coefficient). Large Pe numbers are typical of laminar flows in a microchannel, where diffusive mixing is slow compared with uniaxial convective motion. Mixing of two fluids in an annular microchannel was modelled as a laminar, convection–diffusion problem with two-dimensions (using infinite depth as an ideal limit). This method considers the simultaneous effect of both mass transport elements for the three scaling regimes; low Pe numbers (diffusion dominated), high Pe numbers (convection dominated) and intermediate Pe numbers (the Taylor dispersion regime). Gleeson et al. have provided a comprehensive examination of the mathematical solutions involved [20].

The geometry of the annulus is shown in Fig. 6, where R is the radius of the centre-line and ρ the half width. These dimensions can be related by the non-dimensional parameter $\gamma = \rho/R$, that produces two extremes; a locally straight channel ($\gamma \rightarrow 0$) and a punctured disc ($\gamma \rightarrow 1$). In this

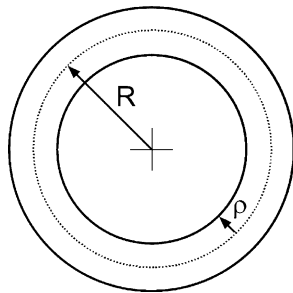


Fig. 6. Annular geometry, showing the centre-line radius R and the channel half-width ρ .

paper, the velocity is characterised by an average angular velocity ω , and therefore $Pe = \omega R\rho/\kappa$ can be used to define the dispersion in this annular system. During mixing, the total amount of solute remains constant, and as the solute becomes redistributed over the area of the annulus during mixing the deviation of the concentration m decays asymptotically to zero. The deviation of the concentration at a given time t is $m(t)$, and the time required to reduce the deviation of the concentration to a specified value M , is defined as the mixing time T_M (i.e. $m(T_M) = M$). Three different values of M were investigated and the non-dimensionalised mixing time $\kappa T_M/R^2$ (i.e. the mixing time compared to the time needed for purely diffusive mixing) can be plotted against the Peclet number. With this approach, κ can remain fixed while variation of the rotation velocity or channel dimensions can be used to change Pe . This is of particular relevance when defining optimum micromixer dimensions and operating velocities for a given solute and solvent.

Asymptotic analysis was used to understand each of the three scaling regimes and was validated by numerical simulation of the convection–diffusion equation. The diffusion-dominated regime can be determined by neglecting the convective component of the convection–diffusion equation. Conversely, mixing at high Pe numbers involves solving a singular perturbation problem, as the diffusion is much smaller than the convective term. Intermediate Pe numbers can be calculated in terms of the Taylor dispersion in a straight capillary due to convection [21,22], and can be readily adapted to find the dispersion in an annulus [23]. An examination of the Pe numbers for which Taylor's approximations are valid leads us to conclude that for Pe numbers in the range $7.2 \ll Pe \ll 15/\gamma$, the mixing measure has an exponential tail as $t \rightarrow \infty$ with a Taylor dispersion coefficient D . As shown in Fig. 7, the mixing time decreases from the diffusion time through the Taylor regime at a rate proportional to Pe^{-2} , and then continues to decrease at a slower rate beyond the Taylor regime. The slower rate corresponds to $Pe^{-2/3}$ scaling initially, i.e. for $M \geq 0.1$, but is closer to $Pe^{-1/2}$ for very small values of M (well mixed). However, at large time scales for high Pe numbers and low M values, asymptotic analysis no longer accurately describes the time evolution of the concentration deviation predicted by the numerical results. Significantly, the asymptotic predictions remain valid when γ is a sizeable fraction of unity, and for non-symmetrical initial conditions (i.e. when mixing two fluids of differing volume).

The geometry of the micromixer clearly influences the mixing performance. It can be shown that for the small γ ratios likely to be used in practical designs, the Peclet number scales as ρ^3/R for given electric and magnetic fields, and a fixed diffusion coefficient κ . When realistic diffusion coefficients are considered, the associated large Peclet numbers dictate that efficient mixing occurs in the convection-dominated regime. To promote faster mixing it is therefore necessary to operate at still larger Peclet numbers by increasing the convective element of mixing. This

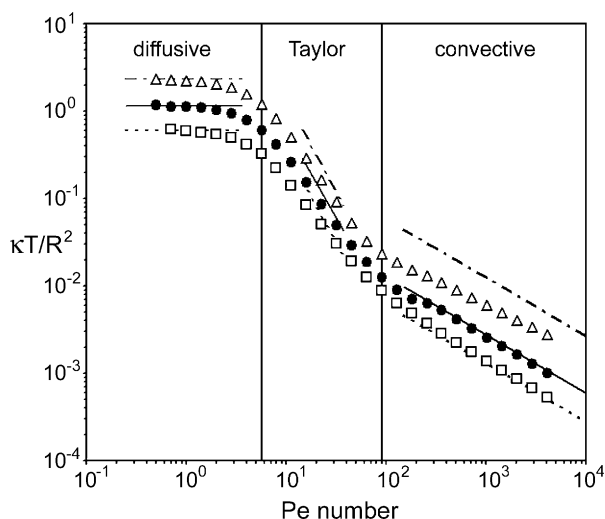


Fig. 7. Mixing times non-dimensionalised by the diffusion time, $\kappa T/R^2$, as a function of the Peclét number, for $\gamma = 0.2$. Asymptotic results are shown in lines, and numerical results as symbols for values of the mixing measure: $M = 0.3$ (dashed line; squares), $M = 0.1$ (solid line; points), and $M = 0.01$ (dot-dash line, triangles).

can be achieved by increasing the channel half-width ρ relative to the centre-line radius R (i.e. by increasing γ). This approach shortens the Taylor regime and imparts higher rotational velocities.

3.3. Micromixing performance

The interfacial area between two initially separated fluids grows during circulation. Annular MHD-mixing of two aqueous streams, originally distinguished by the presence or absence of fluorescein, is depicted at various time intervals in Fig. 8. At high velocities (e.g. 8 mm s^{-1} average) the structuring of high surface area lamellae can be observed for several revolutions when using fluorescein and BPB. The annular channel arrangement provides an infinite length, such that even molecules with small diffusion coefficients can eventually become uniformly mixed. The high diffusion coefficient of the hydrogen ion results in considerably faster mixing with BPB. Here, circulation for approximately one revolution is sufficient for complete homogenisation. This

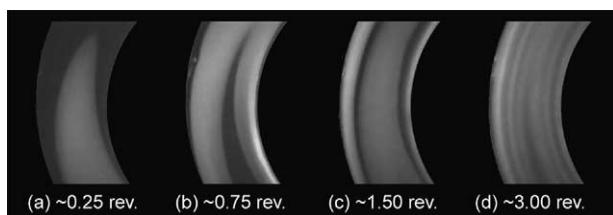


Fig. 8. Frames depicting the evolution of the micromixing conditions in the open machined MHD prototype at an average velocity of 7.7 mm s^{-1} . A 1 M KCl electrolyte is used, and one stream is visualised using fluorescein dye. From left to right, images were recorded during circulation at (a) 0.4, (b) 1.3, (c) 2.8 and (d) 6.3 second intervals, respectively. The peak velocity revolution number is also denoted.

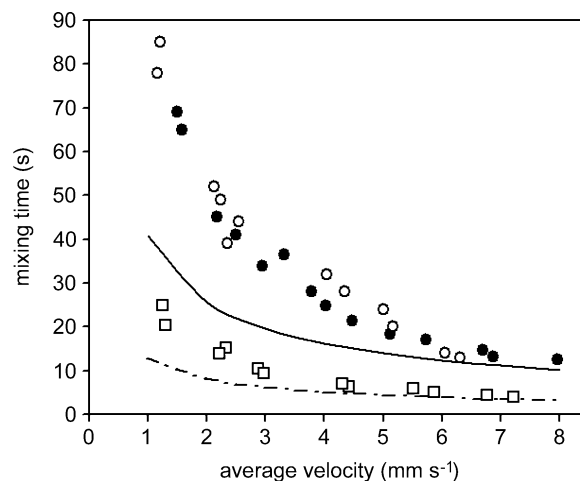


Fig. 9. Micromixing performance of the open machined device. Mixing time plotted against average linear velocity. The time required for mixing of $3 \mu\text{L}$ aliquots of fluorescein (solid circles) and BPB (empty circles) and 500 nL aliquots of HCl (squares) within a $32 \mu\text{L}$ MHD-driven stream of 1 M KCl (aq). The asymptotic data with a mixing measure $M = 0.3$ for fluorescein (solid line) and H^+ (dot-dash line) are plotted for comparison.

experiment observes the interaction of hydrogen ions with BPB molecules, and therefore introduces an error for the measured mixing time of H^+ . However, the diffusion coefficient of the hydrogen ion is ~ 30 -fold higher than that of BPB, and the diffusive component of the mixing process is therefore dominated by the mobility of the hydrogen ion. Plotted in Fig. 9, the mixing times for the homogenisation of fluorescein, BPB, and H^+ with BPB are recorded for various velocities in the open machined device, and compared with values generated by the asymptotic model.

As anticipated the mixing times for fluorescein and BPB were found to be similar while the mixing times for the hydrogen ion are significantly less, approximately three-fold faster under the same actuation conditions. The mixing times for the asymptotic data with a mixing measure $M = 0.3$ compare favourably with the experimental data. To gain a better understanding of the annular mixing behaviour the model mixing times for the three mixing measures ($M = 0.3, 0.1$ and 0.01) are plotted with the experimental data in Fig. 10 in terms of the non-dimensionalisations $\kappa T/R^2$ and Peclét number. It is evident that mixing occurs in the convective regime for the velocities and geometry considered here. The graph also indicates that the experimental method introduces a mixing measure M of 0.1 for low Peclét numbers and a given solute. For higher Peclét numbers (higher velocities) and the same solute the mixing measure becomes $M = 0.3$. Observation of the concentration deviation throughout the entire annulus could be used to curb this change in the mixing measure. Moreover, automation of the experimental protocol can be used to reduce measurement errors. Further modelling to include three dimensional effects may also reveal slightly different scaling behaviour.

The micromachined silicon device was also capable of micromixing, and for typical velocities achieves mixing in

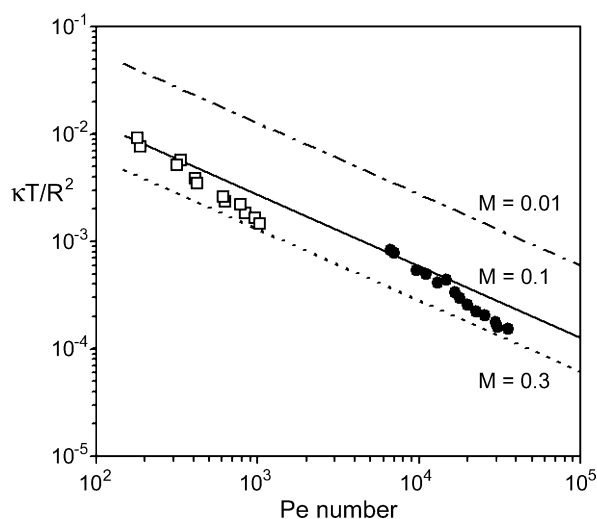


Fig. 10. Convective regime mixing times non-dimensionalised by the diffusion time, $\kappa T/R^2$, as a function of the Peclet number, for $\gamma = 0.2$. Asymptotic results are shown in lines for values of the mixing measure: $M = 0.3$ (dashed line), $M = 0.1$ (solid line), and $M = 0.01$ (dot-dash line). The experimental mixing times for fluorescein (solid circles) and H^+ (empty squares) are plotted for comparison.

the convective regime. However, the scaling behaviour of MHD propulsion and the imposed electrolysis limits associated with the silicon device retard velocity capabilities and have profound implications for micromixing. A single revolution, at the peak transport velocity, takes ~ 55 s when operating close to the velocity limit, producing mixing times of ~ 1.5 min. Clearly, methods to increase fluid velocity are required.

An increased magnetic field will allow higher velocities to be attained. By separating the electromagnet from the channel electrodes in the circuit the voltage limits dictated by electrolysis are no longer imposed. This allows higher magnetic fields to be realised and, when using a phase controller to synchronise electric and magnetic fields, significant velocity gains can be achieved. Furthermore, an additional electromagnet can be placed above the channel to concentrate the magnetic flux and produce an extra four-fold increase in the field. This approach can be simulated with Maxwell 2-D Field Simulator (Ansoft), and

when using 1 A at 1 kHz a magnetic field of the order of 200 mT is predicted. Simple calculation reveals that average transport velocities of ~ 5.5 mm s^{-1} , or average revolution times of < 6 s, can be attained with the silicon micropump when using a magnetic field of this magnitude. However, this method also introduces a four-fold increase in the inductance and associated voltage requirements.

The channel geometry can also be altered to provide improved mixing performance. MHD propulsion effectively scales with h^2 . Deeper channels, approaching the dimensions of the channel width, can therefore be used to attain considerably higher actuation velocities. The fabrication of deep structures in glass or silicon requires alternative processing methods such as deep reactive ion etching (DRIE) or advanced silicon etching (ASE). Other possibilities include the use of co-fired ceramic tapes [24] or powder blasting [25] to realise channels with depths in excess of 500 μm . Annular MHD microreactors with these dimensions can be used to affect the mixing of μL in seconds rather than nL in microseconds. Although this represents a step away from miniaturisation, it is recognised that large volumes of the order of tens of μL are desirable for bulk chemical synthesis or for certain analytical scenarios where small volumes create a sampling problem. Despite the implied dimensions, the benefits of miniaturisation are still relevant.

3.4. Lateral partitioning

The ability to circulate laminar streams using annular MHD actuation can be used to increase the interfacial area in accordance with the behaviour predicted by modelling. This method assumes that the viscosity and density terms in the convection–diffusion equation are equal for all streams. However, the introduction of density disparities between streams by unequal KCl doping presents non-ideal conditions for micromixing, where the initial interfacial area growth becomes reversed. Fig. 11 records the sequence of events as the system evolves from a state with a small interfacial area (2 s) to one of a high interfacial area (8 and 13 s), before relaxing to one with a small interfacial area (so-called partitioned—18 s), and finally diffusion

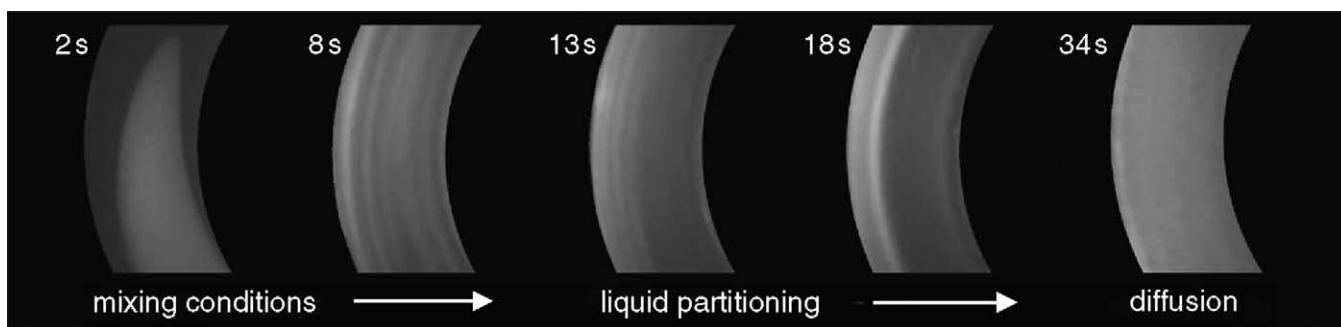


Fig. 11. Sequence of events following the circulation of a 3 μL aliquot of 5 mM fluorescein in double distilled water with a carrier stream of 32 μL of 1 M KCl (1.072 density ratio) with an average velocity of 7.6 mm s^{-1} in the open machined device.

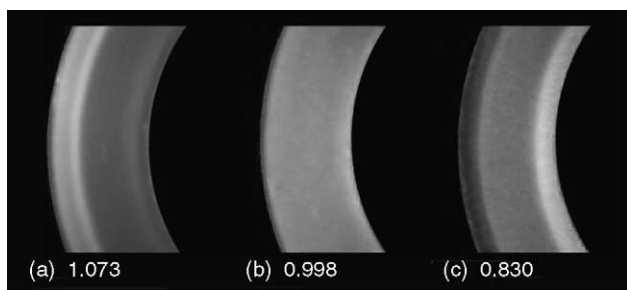


Fig. 12. Frames depicting three experiments following 14 s of actuation at an average velocity of $\sim 8.0 \text{ mm s}^{-1}$ in the open machined device. From left to right, experiments entail the circulation of (a) 5 mM fluorescein with 1 M KCl, (b) 5 mM fluorescein in 1 M KCl with 1 M KCl, and (c) 5 mM fluorescein in 3 M KCl with 250 mM KCl. For each experiment and during circulation the fluorescein dye becomes partitioned to the left with minimal mixing (a), well mixed (b), and partitioned to the right with minor mixing (c). The carrier:dye density ratios are noted beneath each frame.

dominates to realise a state where the tracer is uniformly distributed across the channel (34 s).

The partitioning behaviour impedes the homogenisation of the solute and differences in the streams' densities (electrolyte concentrations) must be avoided for efficient mixing. In an effort to understand the lateral partitioning process a series of experiments using streams with different electrolyte concentrations, and distinguished using fluorescein, were undertaken. Fig. 12 compares the behaviour of MHD flows with three different density ratios, denoted as carrier:dye density ratios (i.e. H_2O with or without KCl: H_2O with fluorescein and with or without KCl). It is evident that the observed partitioning phenomenon arises as a consequence of differing quantities of electrolyte within each aqueous stream. Here, the densest phase collects towards the inner channel wall and not the outer channel wall as would be expected with centrifugation. Further analysis reveals that the partitioned state (defined as a single 2-D interface about the channel's circumference) evolves after approximately 4.5 revolutions at average velocity. High fluid velocities are therefore necessary to observe partitioning before diffusion dominates and the electrolyte differences become negligible. Consequently, this behaviour is not observed when using the silicon device at the systems present operational limits. To combat this feature large electrolyte molecules with small diffusion coefficients could be used to maintain inter-stream concentration differences to affect partitioning at lower pumping velocities. This same approach could also be used to achieve more pronounced and lengthy partitioning in high velocity systems.

This simplistic understanding is sufficient for dynamically structuring aqueous streams in a predictable manner. Presently, however, a fundamental appreciation of the partitioning mechanism has not been achieved. The density and conductivity of a liquid stream are two distinct but interrelated characteristics that are associated with the electrolyte concentration. These features are also closely linked with

the MHD pumping mechanism, and this has possible implications for the velocities that the two fluid streams attain once partitioned, and therefore for how the streams become partitioned. To gain an insight it is therefore necessary to distinguish and elucidate the roles of the density, ionic strength and velocity factors at play. This can be achieved using a combination of experimental techniques to monitor cross-channel velocities and the distribution of mass and charge as the partitioned state evolves. In addition, it may be necessary to consider events in three dimensions.

The sequence of events depicted in Fig. 11 suggests that the MHD-driven circulation of multiple fluids in the laminar flow regime could provide additional functionality. For example, the large interfacial areas associated with the micromixing conditions would be suitable for microsystem based phase transfer chemistries where agitation is not possible. The subsequent phase separation (relaxation to a minimal interfacial area) would then serve as an excellent means to select the phase containing the solute of interest. The ubiquitous nature of non-aqueous solvents and phase separations in analytical and synthetic chemistry makes this an interesting avenue for research, and by appropriate addition of electrolyte salts it is feasible to consider the actuation of alternative solvents using MHD. Electroosmotic flow is another electrokinetic transport method that can, for example, be used to mobilise methanol, acetonitrile [26] and tetrahydrofuran [27] by the addition of appropriate charge carriers. A cursory inspection of a range of organic solvents reveals those with qualities that would be desirable for conducting phase transfer chemistries using annular MHD propulsion: organic solvents with a high dielectric constant (and therefore electrolyte capacity) and those with a low viscosity character are obvious candidates for rapid MHD circulation and interfacial area elongation. In addition, immiscible solvent pairings could be circulated indefinitely for large phase transfer yields before relaxing to a naturally separated state. Finally, it is recognised that the channel electrodes can be readily patterned for the localised electrochemical detection of partitioned analyte species. To illustrate this feature, the gold electrodes on the silicon MHD micropumps have been used for the quantitative detection of ferrous cyanide by cyclic voltammetry (data not shown).

4. Conclusions

This study demonstrates the fluid transport capability of MHD actuation. When MHD-driven propulsion is coupled with a microscale annulus laminar flow effects can be used to impart functionality. The circulation of fluid causes the repetitive internalisation of two streams within each other. This technique produces linear in time increases in the interfacial area for efficient mixing by diffusion, and when characterised and modelled reveals asymptotic evolution to the mixed state. The model reveals that faster mixing can be achieved under the same actuation conditions by geometry

alterations to increase the rotational velocity and therefore the convective component of mixing.

A transverse partitioning capability was also observed when mobilising aqueous streams with disparate electrolyte concentrations. This approach could find service as a means to conduct phase transfer chemistries. Indeed, the dynamic and complex structuring of laminar flows by MHD propulsion in a single and simple channel offers great potential for the fields of analytical and synthetic chemistry.

Acknowledgements

The authors gratefully acknowledge Brian Lillis, Joe O'Brien, and Ye Shu-Ren (NMRC) for assistance with fabrication, Peter O'Brien and Alan O'Neill (NMRC) for access to their laboratory resources, Terence O'Donnell (NMRC) for magnetic field simulation, Damien Arrigan (NMRC) for separation chemistry suggestions, and Olivia M. Roche (Department Applied Mathematics, UCC) for assistance with the model. The research was partly supported by the EU under the DISSARM QLK-CT-2000-00765 project, and by funding from Enterprise Ireland's International Collaboration Fund and Science Foundation Ireland.

References

- [1] J.P. Brody, P. Yager, R.E. Goldstein, R.H. Austin, *Biotechnology at low Reynolds numbers*, *Biophys. J.* 71 (1996) 3430–3441.
- [2] N.L. Jeon, S.K.W. Dertinger, D.T. Chiu, I.S. Choi, A.D. Stroock, G.M. Whitesides, Generation of solution and surface gradients using microfluidic systems, *Langmuir* 16 (2000) 8311–8316.
- [3] L. Pollack, M. Tate, N. Darnton, J.B. Knight, S.M. Gruner, W.A. Austin, R.H. Eaton, Compactness of the denatured state of a fast-folding protein measured by submillisecond small angle X-ray scattering, *Proc. Natl. Acad. Sci. U.S.A.* 96 (1999) 10115–10117.
- [4] J.B. Knight, A. Vishwanath, J.P. Brody, R.H. Austin, Hydrodynamic focusing on a silicon chip: mixing nL in microseconds, *Phys. Rev. Lett.* 80 (1998) 3863–3866.
- [5] A.D. Stroock, S.W.W. Dertinger, A. Ajdari, I. Mezic, H.A. Stone, G. Whitesides, Chaotic mixer for microchannels, *Science* 295 (2002) 647–651.
- [6] H.H. Bau, J. Zhong, M. Yi, A minute magneto hydro dynamic (MHD) mixer, *Sens. Actuators, B, Chem.* 79 (2–3) (2001) 207–215.
- [7] M.H. Oddy, J.G. Santiago, J.C. Mikkelsen, Electrokinetic instability micromixing, *Anal. Chem.* 73 (2001) 5822–5832.
- [8] S.C. Jacobson, T.E. McKnight, M.J. Ramsey, Microfluidic devices for electrokinetically driven parallel and serial mixing, *Anal. Chem.* 71 (1999) 4455–4459.
- [9] C. Erbacher, F.G. Bessoth, M. Busch, E. Verpoorte, A. Manz, Towards integrated continuous-flow chemical reactors, *Mikrochim. Acta* 131 (1999) 19–24.
- [10] A.V. Lemoff, A.P. Lee, An AC magnetohydrodynamic micropump, *Sens. Actuators, B, Chem.* 63 (2000) 178–185.
- [11] J. West, B. Karamata, B. Lillis, J.P. Gleeson, J. Alderman, J.K. Collins, W. Lane, A. Mathewson, H. Berney, Application of magnetohydrodynamic actuation to continuous flow chemistry, *Lab. Chip* 2 (4) (2002) 224–230.
- [12] N. Leventis, X. Gao, Magnetohydrodynamic electrochemistry in the field of Nd-Fe-B magnets. Theory, experiment, and application in self-powered flow delivery systems, *Anal. Chem.* 73 (2001) 3981–3992.
- [13] A.V. Lemoff, A.P. Lee, An AC magnetohydrodynamic microfluidic switch, *Proceedings μ TAS-2000*, Enschede, The Netherlands, 2001, pp. 571–574.
- [14] H.H. Bau, J. Zhu, S. Qian, Y. Xiang, A magneto-hydrodynamically controlled fluidic network, *Sens. Actuators, B, Chem.* 88 (2003) 205–216.
- [15] K.M. Grant, J.W. Hemmert, H.S. White, Magnetic field-controlled microfluidic transport, *J. Am. Chem. Soc.* 124 (3) (2002) 462–467.
- [16] J. O'Brien, P.J. Hughes, M. Brunet, B. O'Neill, J. Alderman, B. Lane, A. O'Riordan, C. O'Driscoll, Advanced photoresists technologies for microsystems, *IOP J. Micromech. Microeng.* 11 (4) (2001) 353–358.
- [17] J.P. Gleeson, J. West, Magnetohydrodynamic micromixing, in: *Proceedings of the Fifth International Conference on Modelling and Simulation of Microsystems (MSM2002)*, Puerto Rico, April 2002.
- [18] J.A. Shercliff, *A Textbook of Magnetohydrodynamics*, Pergamon Press, Oxford, 1965.
- [19] G. Kemp, Capillary electrophoresis: a versatile family of analytical techniques, *Biotech. Appl. Biochem.* 27 (1998) 9–17.
- [20] J.P. Gleeson, O.M. Roche, J. West, A. Gelb, Modelling annular micromixers, *SIAM J. Appl. Math.* (2003), in press.
- [21] G.I. Taylor, Dispersion of soluble matter in solvent flowing slowly through a tube, *Proc. R. Soc. Lond. A* 219 (1954) 186–203.
- [22] R.F. Probstein, *Physicochemical hydrodynamics*, 2nd Edition, Wiley, New York, 1994.
- [23] R.J. Nunge, T.S. Lin, W.N. Gill, Laminar dispersion in curved tubes and channels, *J. Fluid Mech.* 51 (1972) 363–383.
- [24] H.H. Bau, G.K. Ananthasuresh, J.J. Santiago-Aviles, J. Zhong, M. Kim, M. Yi, P. Espinoza-Vallejos, Ceramic tape-based systems technology, *Micro-Electro-Mech. Syst. (MEMS)* 66 (1998) 491–498.
- [25] E. Belloy, S. Thurre, E. Walckiers, A. Sayah, M.A.M. Gijs, The introduction of powder blasting for sensor and microsystem applications, *Sens. Actuators, A, Phys.* 84 (2000) 330–337.
- [26] H. Salimi-Moosavi, T. Tang, D.J. Harrison, Electroosmotic pumping of organic solvents and reagents in microfabricated reactor chips, *J. Am. Chem. Soc.* 119 (1997) 8716–8717.
- [27] G.M. Greenway, S.J. Haswell, D. O'Morgan, V. Skelton, P. Styring, The use of a novel microreactor for high throughput continuous flow organic synthesis, *Sens. Actuators, B, Chem.* 63 (2000) 153–158.

Biographies

Jonathan West received his degree in Medical Microbiology in 1997 from the University of Edinburgh, Scotland. This was followed by research into the genetics of host pathogen interactions using the CF model in the Microbiology Department, University College Cork, Ireland (1997–1998). In 1998, he joined the National Microelectronics Research Centre (NMRC) in Cork, Ireland to undertake his PhD concerning microsystems for genetic analysis. This research programme is ongoing, and has involved the development of methodologies and microfabricated apparatus for sample preparation. To complement these activities, a DNA hybridisation detection format based on capacitance monitoring was also examined. His current research interests include the use of microfluidics to impart analytical and synthetic functionality, and the development of a microfabricated platform for proteomic investigations using optical methods.

James P. Gleeson graduated from University College Dublin in 1994 with a BSc in Mathematical Science, and in 1995 with an MSc in Mathematical Physics. He travelled to Caltech as a Fulbright scholar, and received his PhD in 1999, winning the W.P. Carey prize for best doctoral dissertation in Applied Mathematics. His PhD research was on the application of stochastic processes to model dispersion in turbulent flows. After a year as a visiting assistant professor at Arizona State University, he returned to Ireland as a research fellow in the NMRC and University College Cork. He is currently a member of the department of Applied

Mathematics at University College Cork, where his research interests include random differential equations, and analytical and computational modelling of microsystems and microfluidics.

John C. Alderman received a BSc in Chemistry at Bristol University in 1978, and an MSc in Microelectronics from Bangor College, University of Wales in 1982 while working as a Research Scientist with Plessey Research Caswell, UK. After 12 years with Plessey Research developing processes for IC fabrication he joined the NMRC in 1990 where he initially continued to perform SOI (Silicon on Insulator) based research. Until the end of 2000 and over the preceding 8 years he has collaborated on the development of microsystem-based “smart sensors” for chemical and biological sensing applications. Themes central to this line of work included design, fabrication, packaging, and sensor principles and devices. From the beginning of 2001 he has started to set up a new ‘Bionics’ activity in the NMRC specifically looking at the possibilities to be derived from direct interaction between the cellular and microelectronic worlds. He has published over 80 research papers as sole or joint author in the various fields of work and has several patents filed.

John K. Collins received a BSc in Biochemistry and Microbiology from University College Cork, Ireland in 1970 and a PhD from the same university in 1974. He then worked as a post-doctoral research fellow in the Departments of Anatomy and Pharmacology in Case Western University Medical School, Cleveland, OH (1974–1975) and then to another

position in the Department of Microbiology in the State University of New York (1975–1976). From 1976 until 1978 he worked in the Department of Bacteriology and Pathology at the University of California. In 1978, he returned to Ireland to lecture and develop his cancer research group in the Microbiology Department in University College Cork. He was president of the Irish Association for Cancer Research (1983–1993) and a council member of the European Association for Cancer Research (1985–1993). At present he is Associate Professor of Medicine and Microbiology in University College Cork. His research interests include inflammatory bowel disease, human tumour biology and immunology, virology and sensing systems for medicine. He has in excess of 60 peer-reviewed publications.

Helen Berney graduated with a BSc in Biotechnology from Dublin City University in 1991. She then joined the Cancer Research Campaign Laboratory, Nottingham, England where she worked on a treatment for asthma based on the development of antibodies active against dust mites. In 1993, she joined the NMRC to work on her PhD and as part of a team developing capacitance-based immunosensors. She then went on to continue research on the study of biological and chemical sensors for environmental and medical monitoring. In 2001, she became leader of the NMRC Bioanalytical Microsystems team, with efforts focused on the development of complete genetic analysis systems using microtechnology. She has recently returned from a sabbatical at IBM, Zurich, where she worked on applications for microfluidic networks.